NANO small MICRO

Supporting Information

for *Small*, DOI: 10.1002/smll.201703454

A Lithium–Air Battery Stably Working at High Temperature with High Rate Performance

Jian Pan, Houpu Li, Hao Sun, Ye Zhang, Lie Wang, Meng Liao, Xuemei Sun, and Huisheng Peng**

Supporting Information

A lithium-air battery stably working at high temperature with high rate performance

Jian Pan[†], Houpu Li[†], Hao Sun, Ye Zhang, Lie Wang, Meng Liao, Xuemei Sun, Huisheng Peng**

J. Pan, H. Li, H. Sun, Y. Zhang, L. Wang, M. Liao, Dr. X. Sun, Prof. H. Peng
State Key Laboratory of Molecular Engineering of Polymers, Department of Macromolecular Science, and Laboratory of Advanced Materials, Fudan University, Shanghai 200438, China; E-mail: sunxm@fudan.edu.cn, penghs@fudan.edu.cn.

[†]*These authors contributed equally to this work.*

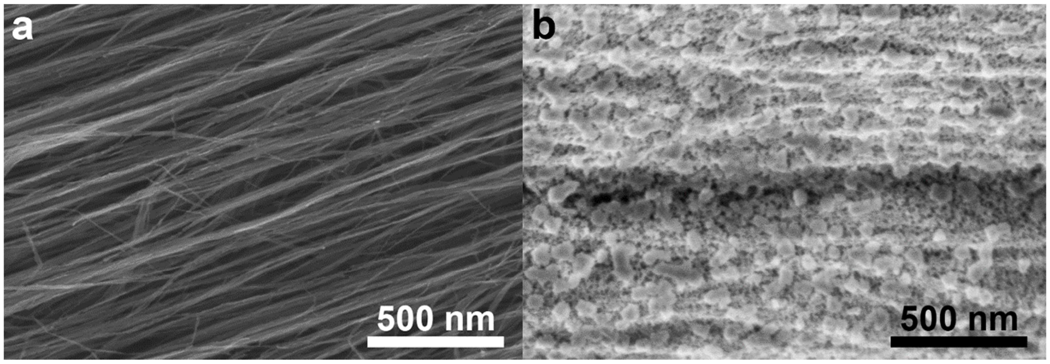

Figure S1. SEM images of the CNT sheets of a) pristine and b) discharged cathode.

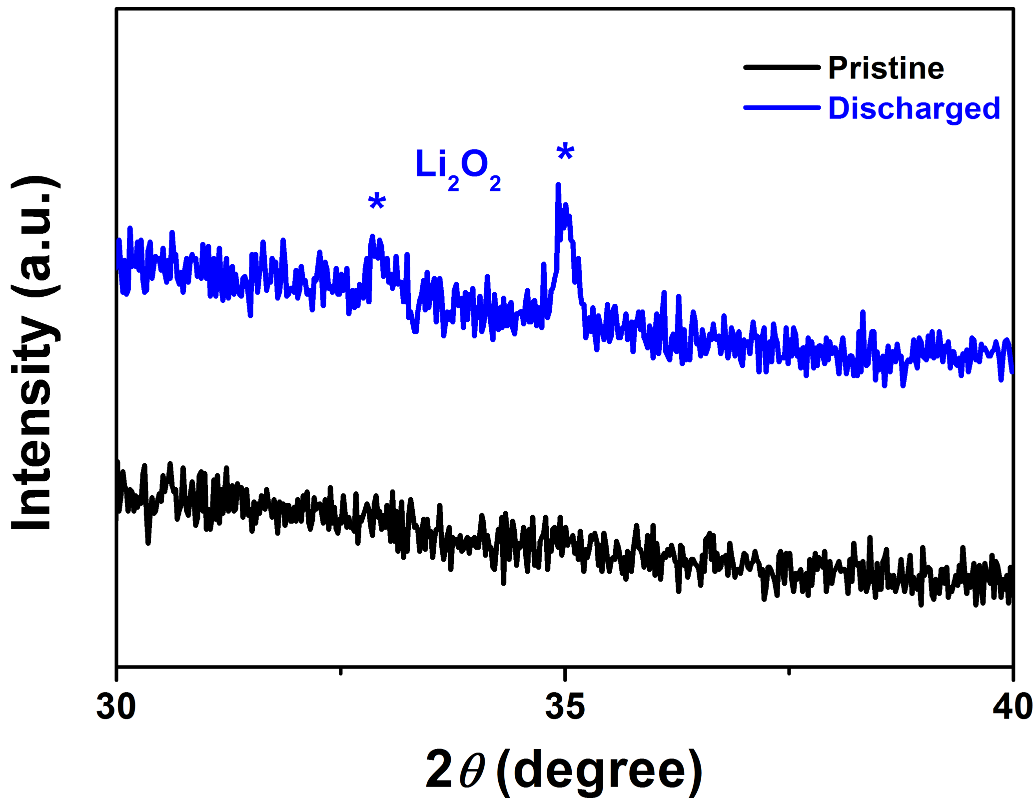

Figure S2. XRD patterns of the pristine and discharged cathode.

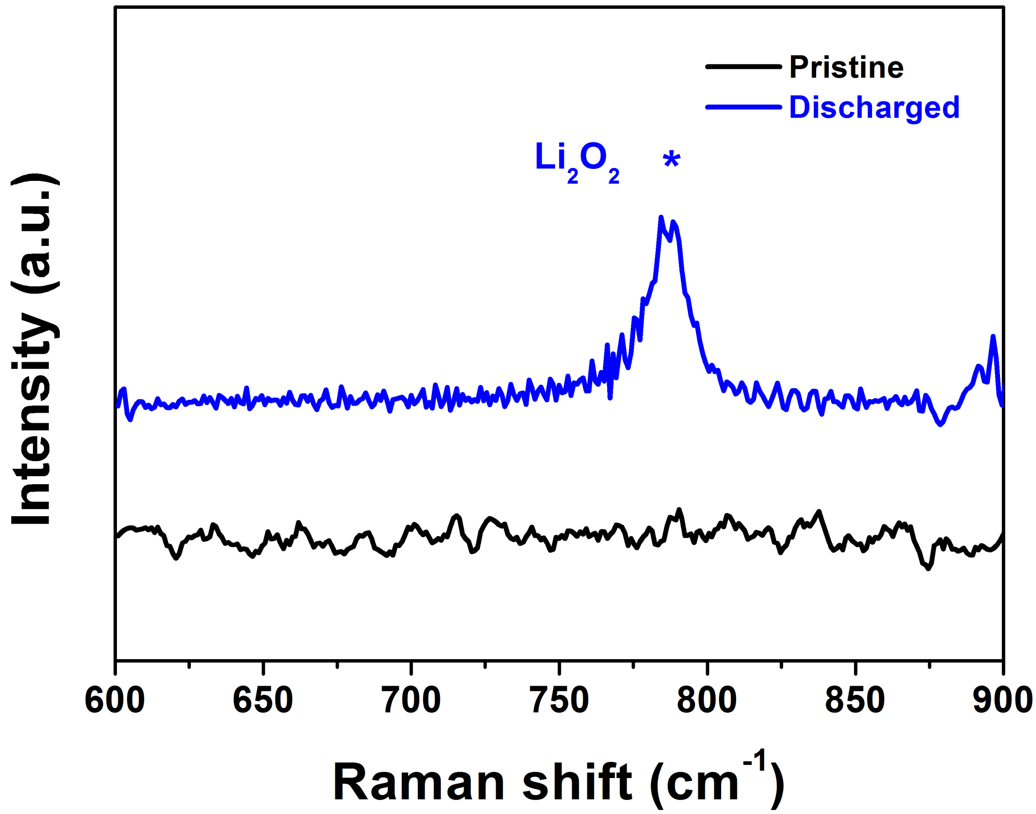

Figure S3. Raman spectra of the pristine and discharged cathode.

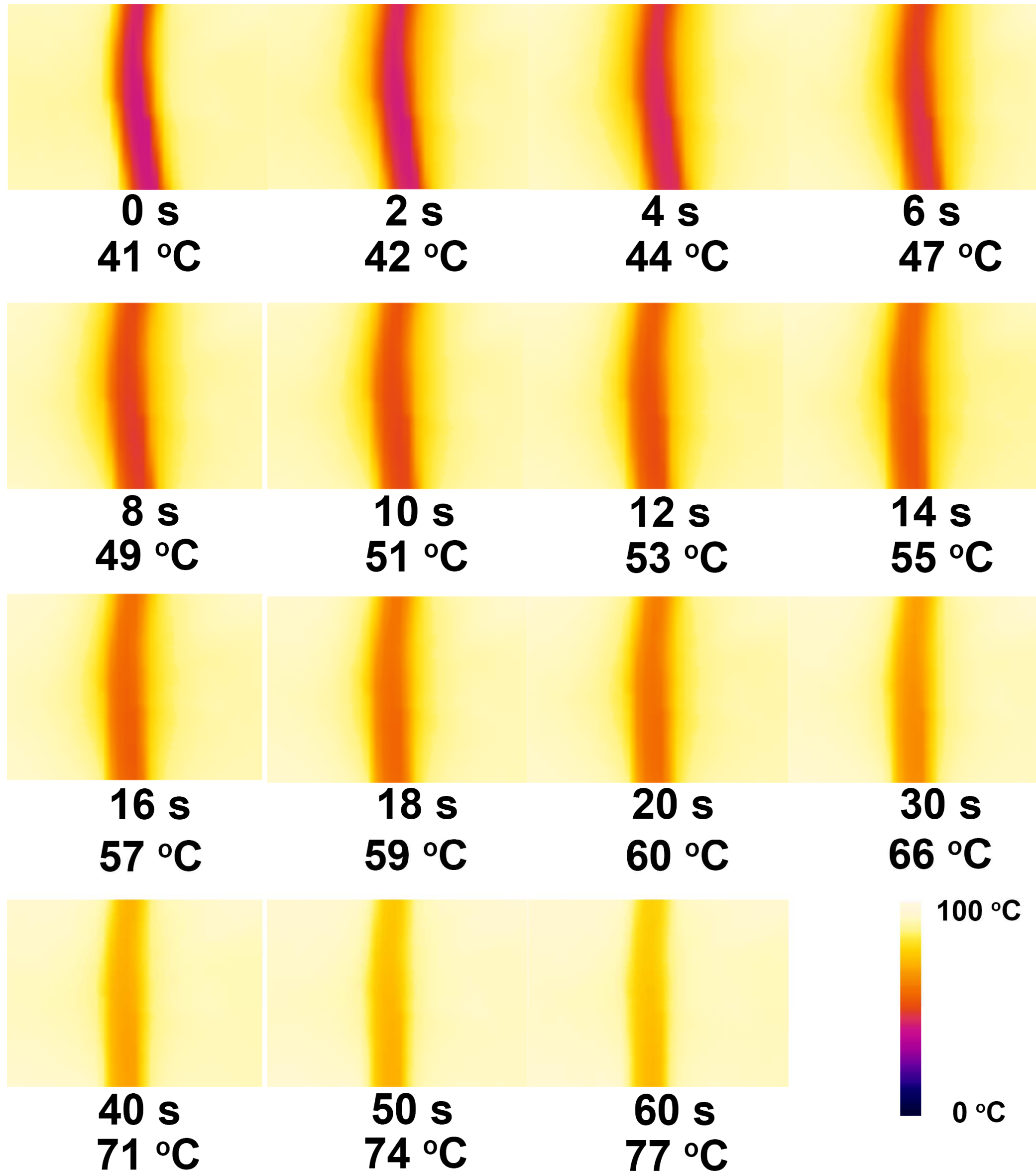

Figure S4. Thermographs of the lithium-air battery under heating.

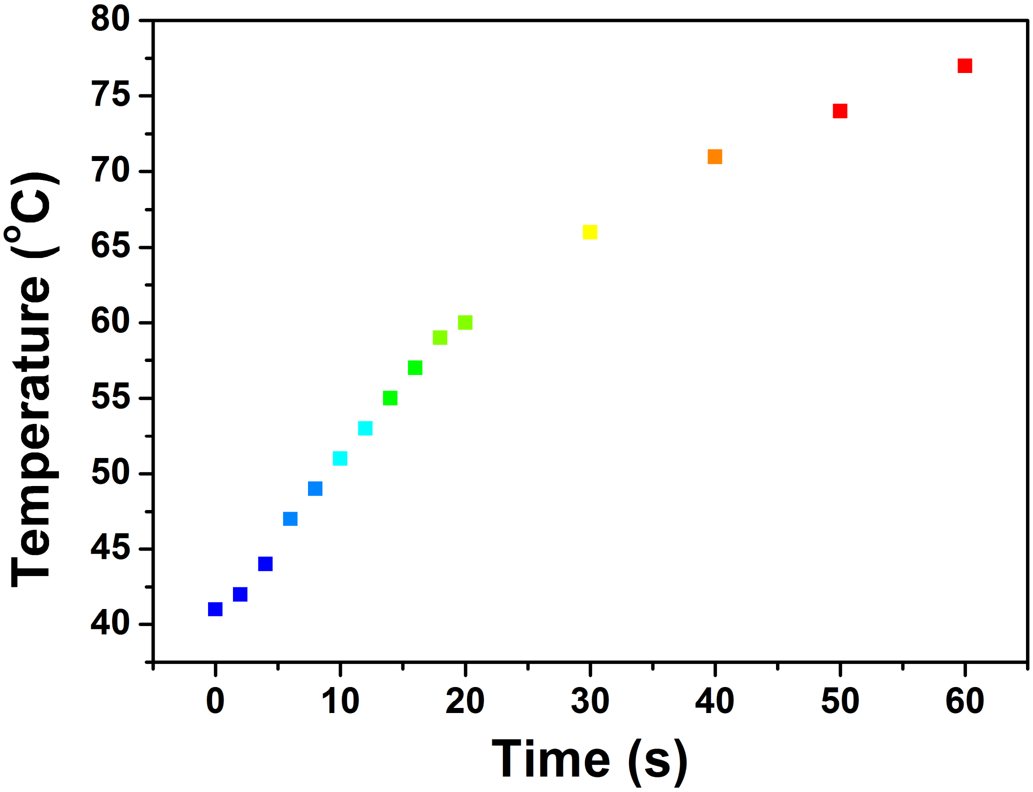

Figure S5. The temperature increase of the lithium-air battery during heating.

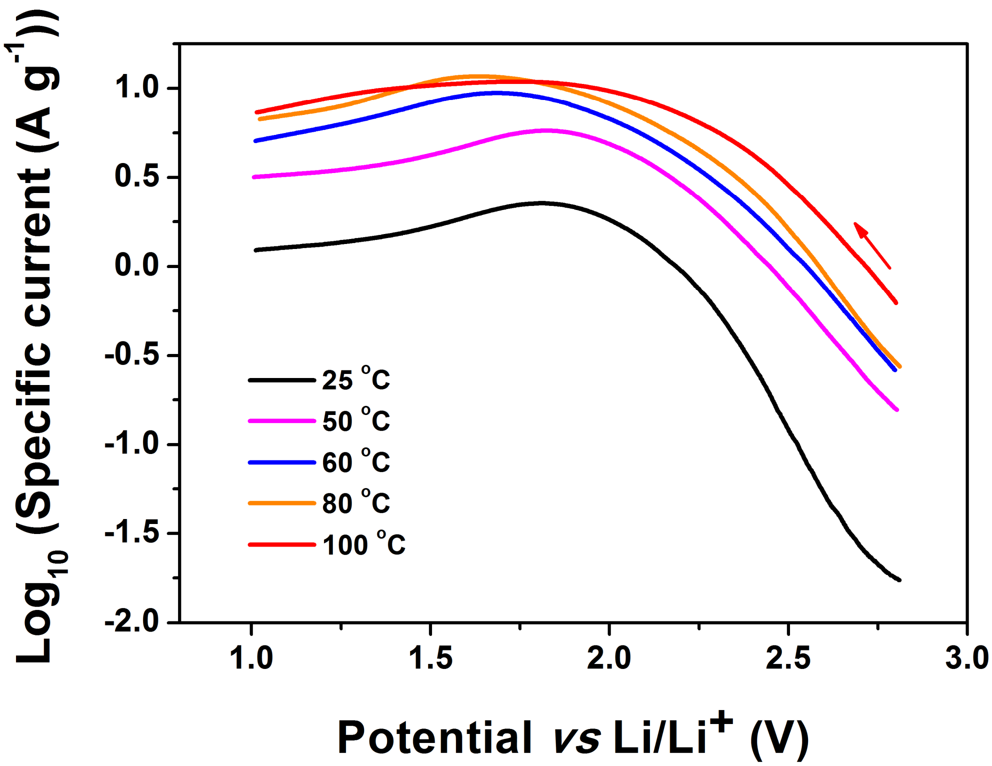

Figure S6. Tafel plots of the air electrode (cathode) at different temperatures during the reduction reaction (Li/Li^+ used as counter and reference electrode).

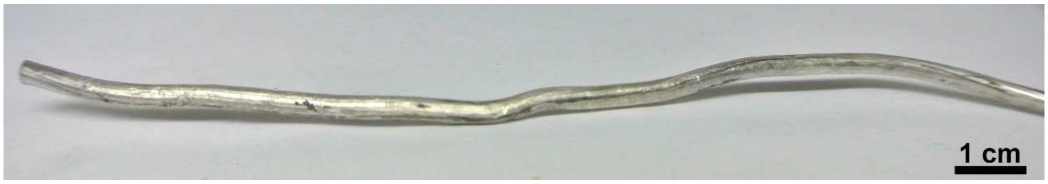

Figure S7. Photograph of a lithium wire.

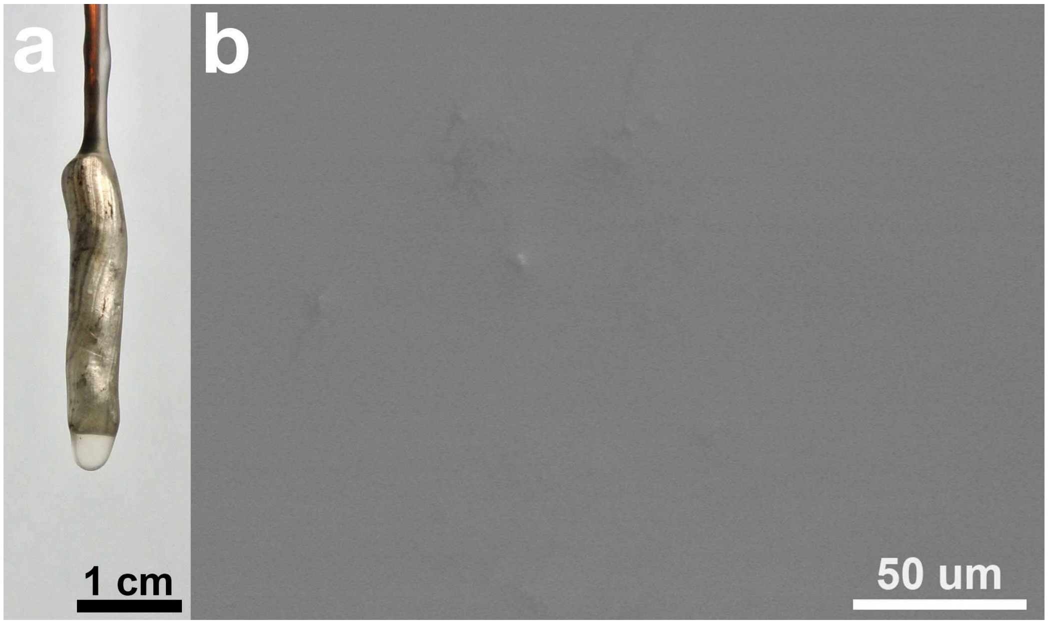

Figure S8. a) Photograph of the ionic liquid gel electrolyte covering on a lithium wire and b) SEM image of the gel electrolyte.

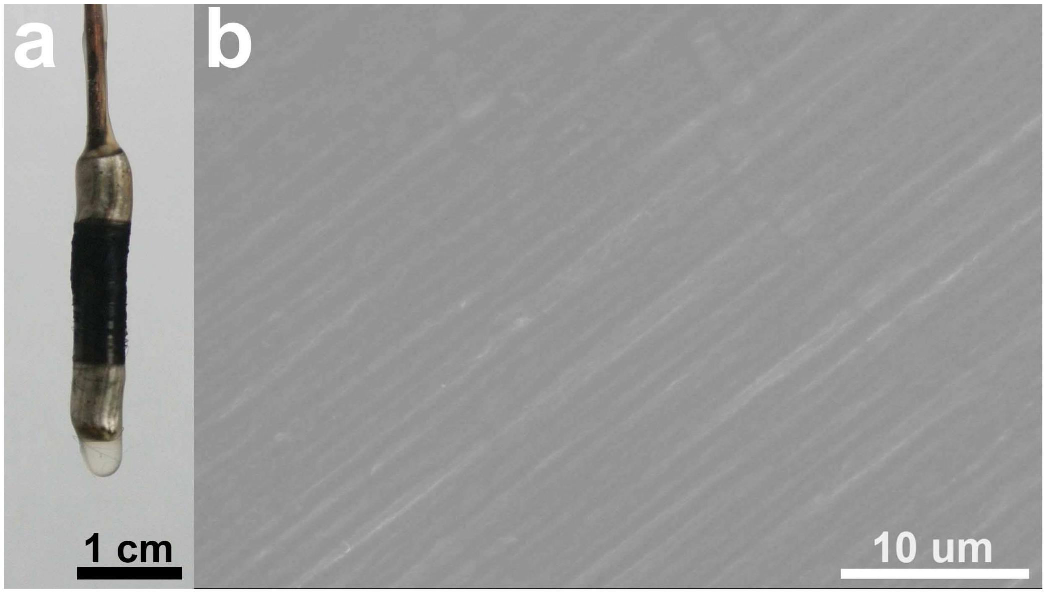

Figure S9. a) Photograph of the aligned CNT sheet-wrapped lithium-air battery and b) SEM image of the surface of the aligned CNT sheet.

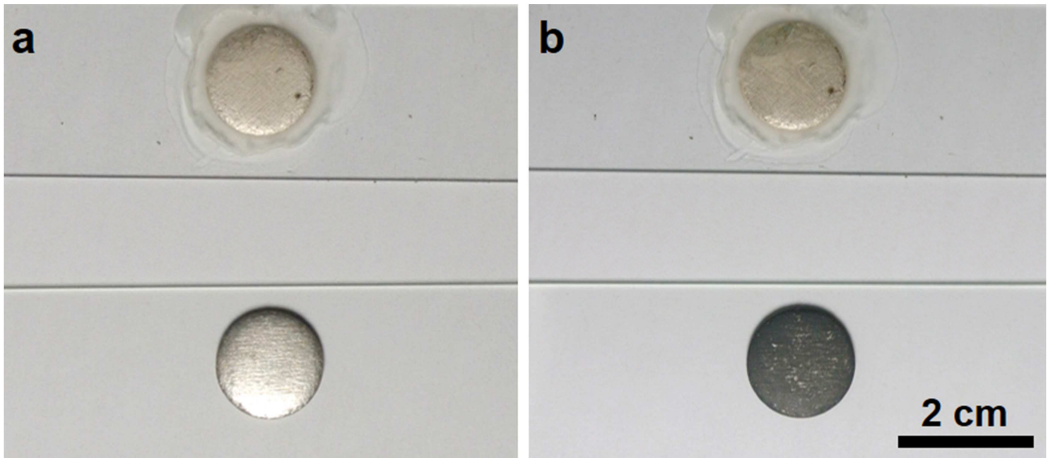

Figure S10. Photographs of a Li foil with (top) and without (down) the coat of ionic liquid gel electrolyte a) before and b) after exposure in air for 30 min.

Table S1. Ionic conductivity of the electrolyte at different temperatures.

Temperature/°C	25	50	60	80	100
Resistance/Ω	32.67	19.25	15.27	12.70	9.42
Ionic conductivity/*10^{-3} S cm^{-1}	0.335	0.568	0.716	0.861	1.16

Calculation example:

The electrolyte used in the stainless steel/electrolyte/stainless steel cell for electrochemical impedance spectroscopy (EIS) was tailored into a round shape with a diameter of 16 mm. The thickness of this round electrolyte film was measured for six times with a vernier caliper:

No.	1	2	3	4	5	6	Average
Thickness/ mm	0.20	0.22	0.22	0.21	0.24	0.23	0.22

Therefore, the average thickness was 0.22 mm.
According to the equation S1:

$$R = \frac{\rho \times l}{S}$$

where R is the resistance, ρ is the electrical resistivity, l is the thickness of the electrolyte film and S is the area of the electrolyte film. Meanwhile, the area can be calculated as:

$$S = \pi \times \left(\frac{D}{2}\right)^2 = \frac{\pi \times D^2}{4}$$

where D is the diameter of the round electrolyte film. Therefore, the ionic conductivity can be figured out as:

$$\rho = \frac{R \times S}{l} = \frac{R \times \pi \times D^2}{4 \times l}$$

In addition, the ionic conductivity can be expressed as:

$$\sigma = \frac{1}{\rho} = \frac{4 \times l}{R \times \pi \times D^2}$$

As a result, at 25 °C, the ionic conductivity was:

$$\sigma = \frac{4 \times 0.22 \times 10^{-3}}{32.67 \times \pi \times (16 \times 10^{-3})^2} = 3.35 \times 10^{-4}\ S\ cm^{-1}$$

For the ionic conductivity at other temperatures, they could be calculated by the same method.

Table S2*. Comparison among different strategies to improve working temperatures in different types of batteries.

Cathode	Anode	Electrolyte	Peak temperature	Battery type	Ref.
$LiCoO_2$/PVDF/conductive carbon (95:2.5:2.5, w/w)	Graphite/PVDF/conductive carbon (95:2.5:2.5, w/w)	1.0 wt% of I_2 in 1.0 M LiPF6 in EC/EMC (1:2, v/v)	90 °C	LIB	[S1]
o-LMO@ Li_2CO_3/PVDF (85:15, w/w)	$Li_4Ti_5O_{12}$-TiO_2 hybrid array	1.0 M LiPF6 in EC/DEC (1:1, v/v)	60 °C	LIB	[S2]
$Li(Ni_xMn_yCo_z)O_2$ (x+y+z=1)	Graphite	4.0 wt% of DPHA: PEGMEM (2:1, w/w) in 1.0 M LiPF6 in EC/DEC (3/7, v/v)	80 °C	LIB	[S3]
$LiMn_2O_4$/PVDF/carbon black (90:5:5, w/w)	Graphite/Super-p/CMC/SBR (95.5:1.0:1.5:2.0, w/w)	Cellulose skeletal incorporated with PECA saturated in 1.0 M LiPF6 in EC/DMC (1:1, w/w)	55 °C	LIB	[S4]
$LiFeO_4$/acetylene black/PVDF (8:1:1, w/w)	Li	3P(MPBIm-TFSI)/LiTFSI/EMIM-TFSI(1/0.3/x)/PVdF-HFP	80 °C	LIB	[S5]
$LiFeO_4$/acetylene black/PVDF (85:5:10, w/w)	Li	poly(bisAEA4)-(0.4 M LiTFSI-MPPipTFSI) (20:80, w/w)	25 °C	LIB	[S6]
(PPy/S/MWCNT (20:70:10, w/w))/PVDF/NMP (80:10:10, w/w)	Lithium foil	1.0 M LiTFSI in DOL/DME(1:1, v/v)	70 °C	Li-S	[S7]
C-S with MLD alucone coating/acetylene black/PVDF (70:20:10, w/w)	Li	1.0 M $LiPF_6$ in EC:DEC:EMC (1:1:1, v/v) 1.0 M LiTFSI in DOL/DME (1:1, v/v)	55 °C	Li-S	[S8]
Pure oxygen/CNT	Li	$P(EO)_{20}$LiTf electrolyte	80 °C	Li-O_2	[S9]
Dry air/aligned CNT	Li wire	(PVDF-HFP/NMP (4:6,	**140 °C**	Li-Air	**This**

	w/w))/(LiTFSI/acetonitrile/BMPy-TFSI (1:1:1, molar ratio)) (4:6, w/w)	**work**

* Abbreviations: PVDF: poly(vinylidene difluoride)

EC: ethylene carbonate

EMC: ethylmethyl carbonate

o-LMO: orthorhombic-$LiMnO_2$

DEC: diethyl carbonate

DPHA: dipentaerythritol hexaacrylate

PEGMEM: poly (ethylene glycol) methyl ether methacrylate

CMC: carboxymethyl cellulose

SBR: styrene butadiene rubber

PECA: poly(ethyl α-cyanoacrylate)

DMC: dimethyl carbonate

3P(MPBIm-TFSI): three-arm imidazolium-based bis(trifluoromethylsulfonyl)imide

EMIM-TFSI: 1-ethyl-3-methylimidazolium bis(trifluoromethylsulfonyl)imide

bisAEA4: ethoxylated bisphenol A diacrylate

MPPipTFSI: N-methyl-N-propylpiperidinium bis(trifluoromethylsulfonyl)imide

PPy: polypyrrole

MWCNT: multi-walled carbon nanotube

NMP: 1-methyl-2-pyrrolidone

LiTFSI: lithium bis(trifluoromethylsulfonyl)imide

DOL: dioxolane

DME: dimethoxyethane

C-S: carbon-sulfur composites

MLD: molecular layer deposited

PVDF-HFP: poly(vinylidene fluoride-co-hexa-fluoropropylene)

BMPy-TFSI: 1-n-butyl-1-methylpyrrolidinium bis (trifluoromethylsulfonyl) imide

Table S3. Performances of different types of batteries with different electrodes, electrolytes and structures.

Battery type	Cathode	Anode	Electrolyte	Structure	Specific energy/Wh $(kg_{cathode})^{-1}$	Specific power/W $(kg_{cathode})^{-1}$	Ref.
Lithium -Ion Battery	LMO@MWCNT	LTO@MWCNT	1M $LiPF_6$/EC+DEC+DMC (1:1:1 w/w)	Fiber	27	880	[S10]
	Functionalized MWCNT	LTO	$LiPF_6$/EC+DMC (3:7 v/v)	Bulk	286.82	22000	[S11]
					372.09	6000	
					387.60	1100	
					403.10	120	
	Reduced graphene oxide	Lithium	1M $LiPF_6$/EC+DMC	Bulk	255.81	22000	[S12]
					348.84	11000	
					403.10	2300	
					705.43	230	
Lithium -Sulphur Battery	Sulphur	Lithium	LITFSI/DME+1,3-DOL+$LiNO_3$ (1 wt%)	Bulk	1845	684.70	[S13]
	Sulphur@TiO_2	Lithium	1 M $LiPF_6$/TEGDME	Bulk	2612.25	709.50	[S14]
					1725.30	1757.25	
					1500.75	3415.5	

Table S4. Performances of lithium-oxygen batteries with different electrodes, electrolytes and structures

Battery type	Cathode	Anode	Electrolyte	Structure	Specific energy/Wh $(kg_{cathode})^{-1}$	Specific power/W $(kg_{cathode})^{-1}$	Ref.
Lithium -Air Battery	α-MnO_2 nanorods @ porous-carbon	Lithium	1 M $LiCF_3SO_3$/TEGDME	Bulk	1194.55	265	[S15]
	Hollow carbon fibers	Lithium	1 M $LiPF_6$/EC:DMC (3:7 v/v)	Bulk	1925.71 1768.56 1481.31	116.10 681.21 1433.44	[S16]
	Aligned CNT	Lithium	LiTFSI+ TMPET /TEGDME+PVDF-HFP	Fiber	3618.05 3436.26	98.43 385.78	[S17]
	Aligned CNT	Lithium	LiTFSI+ TMPET /TEGDME+PVDF-HFP	Fiber	3627.07	388.96	[S17]
	SP	Lithium	1M $LiCF_3SO_3$+ETPTA/TEGDME+PVDF-HFP	Fiber	1993.72	270	[S18]
	Aligned CNT	Lithium	LITFSI/BMPy-TFSI+PVDF-HFP	Fiber	2595.67 1975.24 1389.51	432.30 1225.40 2620.73	**This work 25°C**
	Aligned CNT	Lithium	LITFSI/BMPy-TFSI+PVDF-HFP	Fiber	3719.35 2759.29 2544.77	237.35 6068.10 7884.30	**This work 140 °C**

Discussion:

Since the cathode material is the major concern in the lithium-air battery system, and anode material and electrolyte are always excess in lab experiments, we calculated all the cathode specific power and specific energy based on the weight of cathode materials, i.e., lithium manganese oxide for lithium-ion batteries (LIB), sulfur for lithium-sulfur (Li-S) batteries and carbon materials + oxygen for lithium-air (Li-Air) batteries.[11,15]

A more accurate method would be the integral of voltage multiplies current over discharge, but it is not practical due to lacking of raw data of published reports. In this case, the approximation using voltage plateaus would also give reasonable accuracy.

For the specific capacity (C):

$$C = \frac{I \times t}{m_0}$$

where I is the discharge current, t is the discharge time and m_0 is the weight of the CNT sheet electrode. In this work, $m_0 = 5.04 \times 10^{-5}$ g.

For the specific energy (E) of the lithium-air batteries:

$$E = \frac{I \times t \times U}{m}$$

Where I represents the discharge current, t is the discharge time, U is the discharge voltage plateau and m is the weight of the CNT sheet electrode and reacted oxygen.

For the weight of oxygen (m_{oxygen}): based on the reaction of $2Li + O_2 \rightleftharpoons Li_2O_2$, 1 mol oxygen would be reacted when 2 mol electrons were generated. Therefore, the weight of oxygen m_{oxygen} could be calculated through the following equation:

$$m_{oxygen} = \frac{I \times t \times M_{oxygen}}{2 \times N_A \times e}$$

where I represents the discharge current, t is the discharge time, $M_{oxygern}$ is the molar mass of oxygen, N_A is the Avogadro constant and e is the elementary charge.

For the specific power (P) of the lithium-air batteries:

$$P = \frac{E}{t}$$

where E is the discharge specific energy and t is the discharge time.

Supporting References:

[S1] S.-H. Park, H. J. Kim, J. Jeon, Y. Choi, J.-J. Cho, H. Lee, *ChemElectroChem* **2016**, *3*, 1915.

[S2] J. Guo, Y. Cai, S. Zhang, S. Chen, F. Zhang, *ACS Appl. Mater. Inter.* **2016**, *8*, 16116.

[S3] B. Park, C. h. Lee, C. Xia, C. Jung, *Electrochim. Acta* **2016**, *188*, 78.

[S4] P. Hu, Y. Duan, D. Hu, B. Qin, J. Zhang, Q. Wang, Z. Liu, G. Cui, L. Chen, *ACS Appl. Mater. Inter.* **2015**, *7*, 4720.

[S5] M. Que, Y. Tong, G. Wei, K. Yuan, J. Wei, Y. Jiang, H. Zhu, Y. Chen, *J. Mater. Chem. A* **2016**, *4*, 14132.

[S6] I. Stepniak, E. Andrzejewska, A. Dembna, M. Galinski, *Electrochim. Acta* **2014**, *121*, 27.

[S7] M. Kazazi, *Ionics* **2016**, *22*, 1103.

[S8] X. Li, A. Lushington, Q. Sun, W. Xiao, J. Liu, B. Wang, Y. Ye, K. Nie, Y. Hu, Q. Xiao, R. Li, J. Guo, T.-K. Sham, X. Sun, *Nano Lett.* **2016**, *16*, 3545.

[S9] M. Balaish, E. Peled, D. Golodnitsky, Y. Ein-Eli, *Angew. Chem. Int. Ed.* **2015**, *54*, 436.

[S10] J. Ren, Y. Zhang, W. Bai, X. Chen, Z. Zhang, X. Fang, W. Weng, Y. Wang, H. Peng, *Angew. Chem. Int. Ed.* **2014**, *126*, 7998.

[S11] X. Cui, J. Chen, T. Wang, W. Chen, *Sci. Rep.* **2014**, *4*, 5310.

[S12] B. Z. Jang, C. Liu, D. Neff, Z. Yu, M. C. Wang, W. Xiong, A. Zhamu, *Nano Lett.* **2011**, *11*, 3785.

[S13] X. Ji, S. Evers, R. Black, L. F. Nazar, *Nat. Commun.* **2011**, *2*, 325.

[S14] Z. Wei Seh, W. Li, J. J. Cha, G. Zheng, Y. Yang, M. T. McDowell, P.-C. Hsu, Y. Cui, *Nat. Commun.* **2013**, *4*, 1331.

[S15] Y. Qin, J. Lu, P. Du, Z. Chen, Y. Ren, T. Wu, J. T. Miller, J. Wen, D. J. Miller, Z. Zhang, K. Amine, *Energy Environ. Sci.* **2013**, *6*, 519.

[S16] R. R. Mitchell, B. M. Gallant, C. V. Thompson, Y. Shao-Horn, *Energy Environ. Sci.* **2011**, *4*, 2952.

[S17] Y. Zhang, L. Wang, Z. Guo, Y. Xu, Y. Wang, H. Peng, *Angew. Chem. Int. Ed.* **2016**, *55*, 4487.

[S18] T. Liu, Q.-C. Liu, J.-J. Xu, X.-B. Zhang, *Small* **2016**, *12*, 3101.